Earthline Journal of Chemical Sciences
E-ISSN: 2581-9003; CODEN: EJCSB4
Volume 13, Number 4, November 2026, Pages 491-505
https://doi.org/10.34198/ejcs.13426.34.491505

Synthesis, characterization, and corrosion inhibition efficacy of a novel nitroimidazole-hydrazone for aluminum in hydrochloric acid: experimental and theoretical insights

Aphouet Aurelie KOFFI*

Laboratoire de Constitution et de Réaction de la Matière, UFR SSMT, Université Félix Houphouët-Boigny, Abidjan-Cocody, 22 B.P. 582 Abidjan 22, Côte d'Ivoire
e-mail: koffiaphouet@yahoo.fr

Mamadou YEO

Laboratoire de Thermodynamique et de Physico-Chimie du Milieu, UFR SFA, Université Nangui Abrogoua, 02 BP 802 Abidjan 02, Côte d'Ivoire

Souleymane COULIBALY

Laboratoire de Constitution et de Réaction de la Matière, UFR SSMT, Université Félix Houphouët-Boigny, Abidjan-Cocody, 22 B.P. 582 Abidjan 22, Côte d'Ivoire.

Simplice KOUDJINA

École Nationale Supérieure des Biosciences et Biotechnologies Appliquées (ENSBBA), Université Nationale des Sciences, Technologies, Ingénierie et Mathématiques (UNSTIM), Abomey, Sogbo-Aliho, Bénin, BP 486 Abomey, Sogbo-Aliho, Bénin

Laboratoire de Physique Chimique-Matériaux et Modélisation Moléculaire (LCP3M), Université d'Abomey-Calavi (UAC), 03 BP 3409 Cotonou, Bénin

Mougo André TIGORI

Laboratoire des Sciences et Technologies de l'Environnement, UFR Environnement, Université JeanLorougnon Guédé, BP 150 Daloa, Côte d'Ivoire

Kouhontehoro COULIBALY

Laboratoire de Constitution et de Réaction de la Matière, UFR SSMT, Université Félix Houphouët-Boigny, Abidjan-Cocody, 22 B.P. 582 Abidjan 22, Côte d'Ivoire

Paulin Marius NIAMIEN

Laboratoire de Constitution et de Réaction de la Matière, UFR SSMT, Université Félix Houphouët-Boigny, Abidjan-Cocody, 22 B.P. 582 Abidjan 22, Côte d'Ivoire

Abstract

This study investigates the potential of a newly synthesised nitroimidazole-hydrazone, 1-(3-nitroimidazo[1,2-a]pyridinyl)-3-(2-hydroxyphenyl)hydrazone, to serve as a high-performance corrosion inhibitor for aluminum in hydrochloric acid. Gravimetric analysis revealed exceptional inhibition efficiency, reaching 91.91% at a low concentration of 10^{-4} mol.L^{-1}. Thermodynamic analysis of the adsorption process suggests a mixed-mode mechanism, involving both physisorption and chemisorption on the aluminum surface. Density functional theory

Received: September 17, 2026; Revised & Accepted: October 30, 2026; Published online: November 16, 2026

Keywords and phrases: aluminum, 1-(3-nitroimidazo[1,2-a]pyridinyl)-3-(2-hydroxylphenyl)hydrazone, gravimetric method, density functional theory (DFT).

*Corresponding author

Copyright © 2026 the Authors

(DFT) calculations provided molecular-level insights into this behavior. The negative value of the fraction of electrons transferred (ΔN) confirms chemisorption facilitated by electron donation from the aluminum surface to the inhibitor molecule. Furthermore, frontier molecular orbital analysis and electrostatic potential mapping reveal that nucleophilic attack sites are broadly distributed across the molecule, whereas electrophilic attack is predominantly localized at the nitro group on the pyridinyl ring. Fukui function analysis identified specific reactive sites, with the N29 atom ($\Delta f_k = 0.069$) being the most susceptible to nucleophilic attack and the O16 atom ($\Delta f_k = -0.102$) to electrophilic attack, underscoring their critical role in the adsorption process. The combined experimental and theoretical results robustly establish 1-(3-nitroimidazo[1,2-a]pyridinyl)-3-(2-hydroxylphényl)hydrazone as an effective green inhibitor whose performance is rooted in its distinct electronic structure.

1. Introduction

The extensive utilization of aluminum and its alloys across numerous sectors is founded upon a suite of advantageous characteristics, notably its low density, high ductility, ready recyclability, and significant corrosion resistance [1-3]. However, the passivity afforded by its native oxide layer is compromised in extreme pH conditions; the film's amphoteric character leads to its dissolution, thereby facilitating corrosion of the metal substrate [1].

The degradation of aluminum and its alloys is dictated by a combination of metallurgical factors, such as alloying elements, and external environmental conditions [4]. When exposed to acidic solutions, aluminum is particularly susceptible to pitting corrosion, a localized attack that results in the irreversible deterioration of its mechanical and physical properties [5, 6].

Metallic corrosion, stemming from the inherent reactivity of metals, imposes significant economic costs worldwide [7]. The scale of material loss is staggering, estimated at 150 million tonnes annually—a figure comparable to one-quarter of global steel production, or five tonnes per second [8]. The corresponding financial impact reaches approximately $2.5 trillion, or 3.5% of global GDP. However, leveraging existing corrosion control methodologies could potentially mitigate 15–35% of this cost, yielding annual savings of $375–875 billion [9, 10].

Acidic solutions are indispensable across numerous industrial sectors for operations such as metal pickling, oil well acidization, and the dissolution of undesirable deposits like scale, rust, and biofilms. Among these, hydrochloric acid is the most employed. Nevertheless, its inherently aggressive character mandates the use of corrosion inhibitors to safeguard metallic infrastructure from dissolution [10-12].

A prerequisite for effective acid corrosion inhibition is molecular adsorption, driven primarily by polar functional groups containing heteroatoms (N, O, S) or unsaturated systems [10, 13]. The inhibitory potency is further amplified by π-electron density from double or triple bonds that interact with the metal surface, leading to a structure-activity relationship where more unsaturation yields stronger inhibition [14]. This synergy of features makes heterocyclic compounds a particularly potent and extensively investigated class of inhibitors [1, 12-19]. Furthermore, their specificity is environment-dependent, exemplified by the preference for sulfur-containing compounds in sulfuric acid and nitrogen-containing ones in hydrochloric acid [1, 20].

The fundamental mechanism for corrosion inhibition entails the adsorption of organic molecules onto the metal surface. These interactions are broadly classified as physical adsorption or chemisorption. The specific mode that prevails is not fixed but is contingent upon several parameters, namely the inherent nature and electrochemical charge of the metal, the structural features of the inhibitory compound, and the specific properties of the surrounding electrolyte [21].

In the context of aluminum protection in acidic media by synthesized organic molecules, a first review [22] catalogued a broad range of corrosion inhibitors, including phthalocyanines, phenol, benzene-1,2,4,5-tetracarboxylic dianhydride, imidazole and its derivatives, Schiff bases, and other nitrogen- and/or sulfur-containing compounds such as phenylhydrazine, urea, thiourea, N-allylthiourea, and thiosemicarbazide. A second review [23], covering research published over the past two decades, reported that the cationic surfactant cetyltrimethylammonium chloride, pyrazole compounds, vanillin, and polyacrylamide also exhibit effective inhibitory properties. More recently, Kouame et al. [24, 25] demonstrated the inhibitory properties of two imidazo[1,2-a]pyridine derivatives, namely 2-(2-(4-chlorobenzylidene)hydrazinyl)-3-nitroimidazo[1,2-a]pyridine and 2-(2-benzylidenehydrazinyl)-3-nitroimidazo[1,2-a]pyridine, both of which showed good inhibition efficiency with concentration- and temperature-dependent behavior. Taken together, these studies highlight the diversity of organic scaffolds explored for aluminum protection in acidic media; however, they also reveal that imidazo[1,2-a]pyridine derivatives remain comparatively underexplored in this context, which motivates the present investigation.

This work investigates the corrosion inhibition performance of a novel imidazo[1,2-a]pyridine derivative, 1-(3-nitroimidazo[1,2-a]pyridinyl)-3-(2-hydroxyphenyl)hydrazone, for aluminum in hydrochloric acid. This molecule was synthesised for the first time by Adingra et al. [26]. Its antifungal activity was studied against *Candida albicans* strain n°396 from the CeDReS collection. To the best of our knowledge, this represents the first study of this specific compound in a corrosion science context.

2. Materials and Methods

2.1. Sample and electrolyte medium preparation

High-purity aluminum rods (99.6%) of 2 mm diameter were sectioned into 1 cm lengths (exposed area = 0,6908 cm^2). The specimens underwent a meticulous pre-treatment procedure, which involved sequential polishing with abrasive paper, degreasing with acetone, rinsing with distilled water, and finally oven-drying at 343 K for 10 minutes [27]. Corrosion tests were performed by immersing a prepared sample in 50 mL of a molar hydrochloric acid solution for one hour at temperature ranging from 303 to 323 K. To evaluate the concentration-dependent efficacy of the inhibitor, solutions containing the compound at concentrations ranging from 2.5×10^{-5} to 10^{-4} M were employed. After the corrosion test, the sample was removed, abundantly rinsed with distilled water, and reweighed with the same balance with a precision of 10^{-4} g. All tests were replicated three times to ensure the reproducibility of the results.

2.2. Synthesis of 1-(3-nitroimidazo[1,2-a]pyridinyl)-3-(2-hydroxyphenyl)hydrazone

A mixture of 2-hydrazino-3-nitroimidazo[1,2-a]pyridine (1 mmol, 1 equiv.) and 2-hydroxybenzaldehyde (1 mmol, 1 equiv.) was dissolved in methanol (5 mL). Two drops of acetic acid were added, and the resulting mixture was heated under reflux for 1 h. After cooling to room temperature, the precipitated product was collected by filtration, dried, and purified by recrystallization in ethanol to afford the desired hydrazone as a yellow powder in 95% yield; m.p.>266 °C (dec.) [28].

^{1}H NMR (300 MHz, DMSO-d_6): δ 11.55 (s, 1H, OH), 11.29 (s, 1H, NH), 9.33 (d, J = 6.8 Hz, 1H, Ar-H), 8.85 (s, 1H, CH=N), 7.81 (ddd, J = 8.5, 7.1, 1.2 Hz, 1H, Ar-H), 7.68 (d, J = 8.8 Hz, 1H, Ar-H), 7.47 (dd, J = 8.0, 1.6 Hz, 1H, Ar-H), 7.36–7.23 (m, 2H, Ar-H), 6.92 (dd, J = 10.3, 4.5 Hz, 2H, Ar-H).

^{13}C NMR (75 MHz, DMSO-d$_6$): δ 157.80, 150.02, 148.89, 146.51, 134.48, 131.62, 130.05, 128.99, 119.82, 119.24, 116.92, 116.01, 115.47.

HRMS (ESI): m/z calcd. for $C_{14}H_{11}N_5O_3Na$ $[M+Na]^+$ 320.0538; found 320.0543.

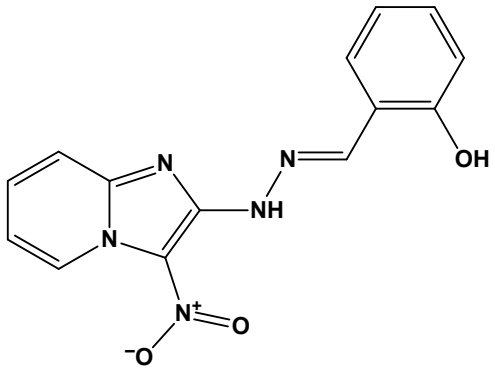


Figure 1. Chemical structure of 1-(3-nitroimidazo[1,2-a]pyridinyl)-3-(2-hydroxyphenyl)hydrazone.

2.3. Gravimetric evaluation of aluminum corrosion inhibition by 1-(3-Nitroimidazo[1,2-a]pyridinyl)-3-(2-hydroxyphenyl)hydrazone in hydrochloric acid

The corrosion rate of aluminum and the inhibitory performance of the target compound were evaluated using a gravimetric technique based on mass loss measurements. Pre-weighed specimens were immersed in the electrolyte for 1 h at temperatures ranging from 303 to 323 K. The corrosion rate (*CR*, in g·cm^{-2}·h^{-1}) was determined using Equation 1, which relates the mass loss (Δm) to the exposed surface area (*S*) and immersion time (*t*).

$$CR = \Delta m/(S \times t) \qquad (1)$$

The inhibition efficiency (*IE*) was subsequently calculated from Equation 2, as a function of the corrosion rates obtained in the absence (CR_0) and presence (CR) of the inhibitor.

$$IE = (CR_0 - CR)/CR_0 \times 100 \qquad (2)$$

2.4. Density functional theory (DFT) study of 1-(3-nitroimidazo[1,2-a]pyridinyl)-3-(2-hydroxylphényl) hydrazone adsorption on aluminum surface

A computational investigation of 1-(3-nitroimidazo[1,2-a]pyridinyl)-3-(2-hydroxylphényl)hydrazone was conducted using the density functional theory (DFT). The molecular structure was built in GaussView 5.0.8 and subjected to pre-optimization, followed by a full geometry optimization with Gaussian 09 W at the B3LYP/6-311 G(d) level [29].

The optimized structure provided both global (E_{HOMO} and E_{LUMO}) and local ($q_k(N)$) reactivity descriptors. A suite of additional parameters was subsequently calculated, including the HOMO–LUMO energy gap, chemical hardness, softness, chemical potential, electronegativity, electrophilicity index, and fraction of transferred electrons, as well as Fukui functions and the dual index.

3. Results and Discussions

3.1. Gravimetric investigation of the corrosion inhibition performance of 1-(3-nitroimidazo[1,2-a]pyridinyl)-3-(2-hydroxyphenyl)hydrazone on aluminum

As shown below (Table 1, Figure 2), 1-(3-nitroimidazo[1,2-a]pyridinyl)-3-(2-hydroxyphenyl)hydrazone caused a dramatic reduction in the corrosion rate at 303 K, from 0.0036 to 0.0003 $g.cm^{-2}.h^{-1}$, with substantial efficacy retained at elevated temperatures (313 K and 323 K).

Table 1. Corrosion rates of aluminium and Inhibitory efficiency of 1-(3-nitroimidazo[1,2-a]pyridinyl)-3-(2-hydroxyphenyl)hydrazone

C_{inh}	Corrosion rate CR ($10^{-3}g.cm^{-2}.h^{-1}$)			Inhibitory efficiency, IE (%)		
($10^{-5}mol.L^{-1}$)	303 K	313 K	323 K	303 K	313 K	323 K
Blank	3.6±0.28	32.5±2.0	58.7±2.9	--	--	--
2.5	1.2±0.23	14.3±1.0	37.5±2.2	67.62	55.93	36.10
5.0	0.6±0.20	9.4±0.7	34.7±2.1	83.81	71.07	40.79
7.5	0.4±0.20	8.3±0.7	29.5±1.8	87.86	74.63	49.67
10.0	0.3±0.20	7.2±0.6	22.6±1.4	91.91	77.97	61.51

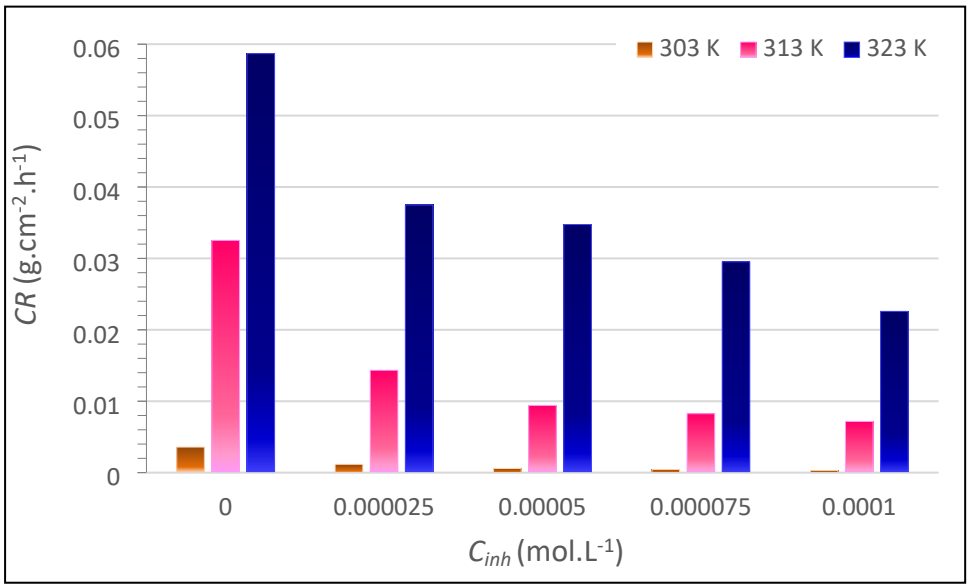


Figure 2. Corrosion rate of aluminum as a function of 1-(3-nitroimidazo[1,2-a]pyridinyl)-3-(2-hydroxylphényl)hydrazone inhibitor concentration across a temperature range of 303–323 K

The results demonstrate that the novel synthesised nitroimidazole-hydrazone protects the substrate in the aggressive environment. Its inhibitory action is attributed to its adsorption onto the aluminum surface, forming a protective barrier. This process is facilitated by molecular interactions involving the compound's heteroatoms and aromatic rings [30]. The stability of this adsorbed layer is evidenced by its persistent performance even at high temperatures. As shown in Table 1 and Figure 3, the inhibition efficiency (E%) of 1-(3-nitroimidazo[1,2-a]pyridinyl)-3-(2-hydroxylphenyl)hydrazone exhibits a strong dependence on both concentration and temperature. The efficiency increased with concentration, achieving a maximum of 91.91% at 10^{-4} M, consistent with the formation of a denser, more effective adsorbed barrier. However, temperature adversely

affected performance; rising temperatures reduced performance, likely due to increased thermal energy that desorbs inhibitor molecules from the metal surface [31]. Importantly, even under these conditions, the inhibitor maintained a robust efficiency of 61.51%, confirming its thermal resilience.

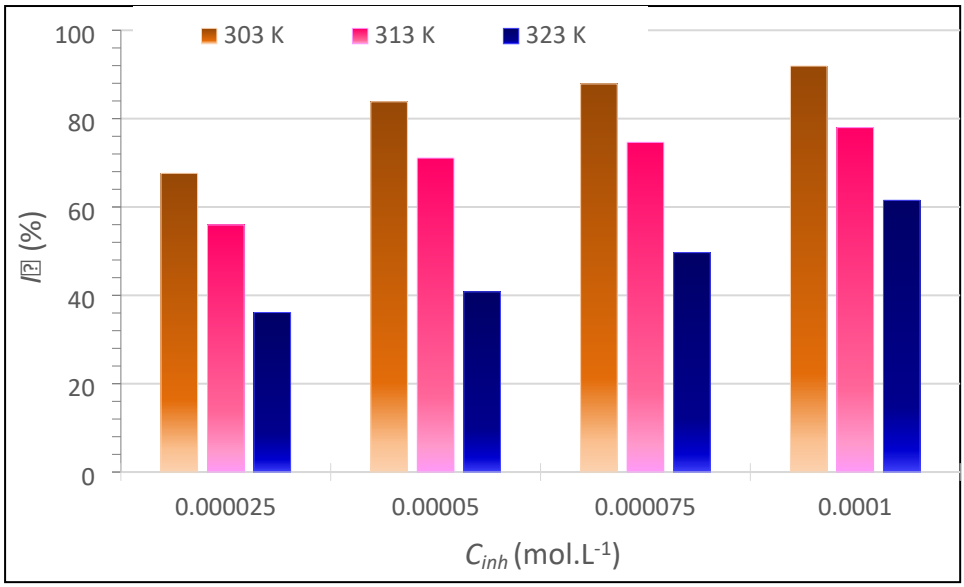


Figure 3. Inhibition efficiency (%E) of the 1-(3-nitroimidazo[1,2-a]pyridinyl)-3-(2-hydroxylphényl)hydrazone inhibitor as a function of its concentration across a temperature range of 303–323 K.

3.2. Adsorption mechanism: isotherm fitting and thermodynamic parameters

The adsorption mechanism of 1-(3-nitroimidazo[1,2-a]pyridinyl)-3-(2-hydroxyphenyl)hydrazone was investigated through isotherm fitting and calculation of the standard Gibbs free energy. Initial fitting to standard isotherms (Table 2) identified the Langmuir model (Figure 4) as the best fit at all temperatures studied based on correlation coefficients, suggesting a homogeneous adsorption scenario [32]. However, the observed deviation of the Langmuir plot slope from unity pointed to non-ideal behavior, likely stemming from intermolecular interactions and multi-site adsorption. To capture these deviations more accurately, the more comprehensive Villamil isotherm, defined by the expression below [33], was subsequently employed.

$$\frac{C_{inh}}{\theta} = \frac{n}{K_{ads}} + nC_{inh} \qquad (3)$$

The spontaneity and nature (physical or chemical) of the inhibitor's adsorption were then evaluated by calculating the standard Gibbs free energy ΔG_{ads} [34]. The following equation was used for this determination:

$$\Delta G_{ads} = -RTLn(55.5\, K_{ads}) \qquad (4)$$

55.5 represents the molar concentration of water, and K_{ads} is the adsorption equilibrium constant.

Table 2. Adsorption isotherm parameters for the adsorption of 1-(3-nitroimidazo[1,2-a]pyridinyl)-3-(2-hydroxyphenyl)hydrazone on aluminum in 1 M HCl.

Isotherm	Parameters	303 K	313 K	323 K
Langmuir	R^2	0.9995	0.9991	0.9154
	Slope	0.9649	1.1233	1.2335
	$K_L(10^3 L.mol^{-1})$	96.490	56.165	24.670
Temkin	R^2	0.9676	0.9601	0.8588
	Slope	0.4011	0.3651	0.3969
	K_T (10^6 L.mol^{-1})	2.093	1.483	0.276
Freundlich	R^2	0.9548	0.9455	0.9027
	Slope	0.2208	0.2398	0.3689
	K_F	7.17	7.27	17.13
El-Awady	R^2	0.9922	0.9752	0.8628
	Slope	1.1878	0.7336	0.7055
	K_{E-A} (10^3)	75.438	59.167	15.200
Dubinin Raduskevich	R^2	0.9717	0.9645	0.8719
	Slope	-0.0041	-0.0043	-0.0062
	K_{DR} (J^{-2} mol^2)	4.1	4.3	6.2

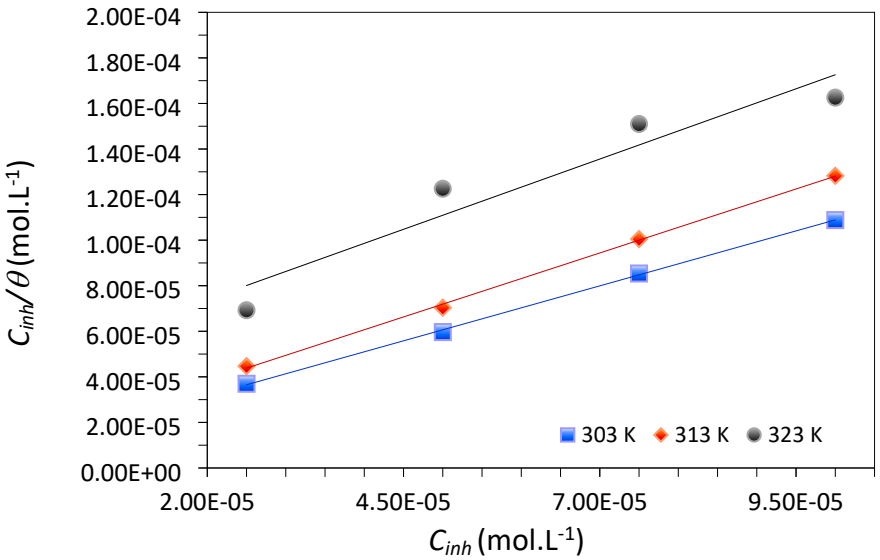


Figure 4. Langmuir adsorption isotherm for 1-(3-nitroimidazo[1,2-a]pyridinyl)-3-(2-hydroxylphényl)hydrazone on the aluminum surface in hydrochloric acid solution

The negative ΔG_{ads} value (Table 3) confirms the spontaneity of the inhibitor's adsorption onto aluminum. The magnitude of ΔG_{ads}, ranging from –39.01 to –37.93 kJ·mol^{-1}, indicates a mixed adsorption mechanism involving both physical and chemical interactions [35, 36].

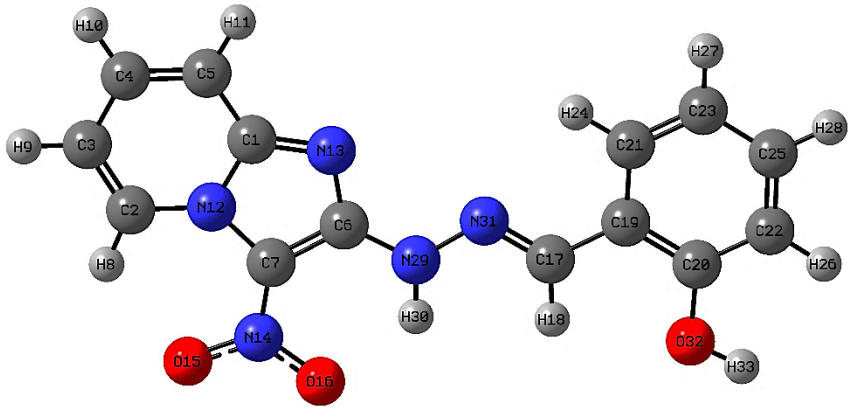
Table 3. Adsorption parameters of 1-(3-nitroimidazo[1,2-a]pyridinyl)-3-(2-hydroxylphényl)hydrazone adsorption onto aluminum surface.

T (K)	K_{ads} (L.mol^{-1})	ΔG_{ads} (kJ.mol^{-1})
303	96490	- 39.01
313	56165	- 38.89
323	24670	- 37.93

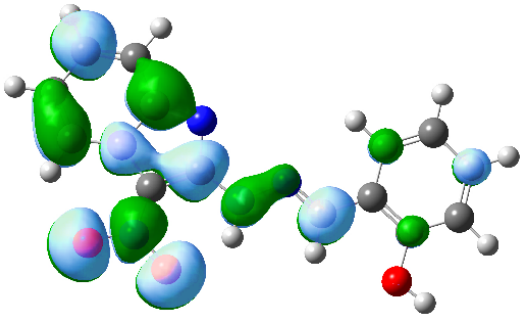
3.3. Insights from density functional theory calculations

Quantum chemical calculations were employed in this study to evaluate key parameters of the molecule under investigation and to propose a mechanism for its inhibitory action. Figure 5 presents the frontier molecular orbitals and electrostatic potential (ESP) maps of the newly synthesized nitroimidazole–hydrazone derivative. Analysis of the orbital distributions reveals that electron density in the HOMO is delocalized over the entire molecular framework. In contrast, the LUMO is predominantly localized on the pyridinyl ring and the adjacent nitrogen atoms. Complementing this, the ESP surface and contour maps facilitate visual identification of nucleophilic (red regions, low ESP) and electrophilic (blue regions, high ESP) sites. Accordingly, nucleophilic attack sites are broadly distributed across the molecule, while electrophilic attack is largely confined to the nitro group on the pyridinyl ring.

Optimized labeled structure

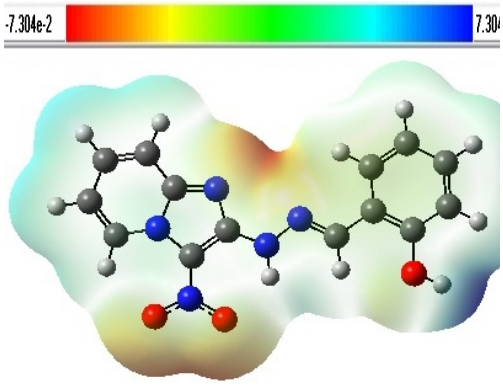


Lowest Unoccupied Molecular Orbital (LUMO)



Highest Occupied Molecular Orbital

Surface map of the electrostatic potential



Contour map of the electrostatic

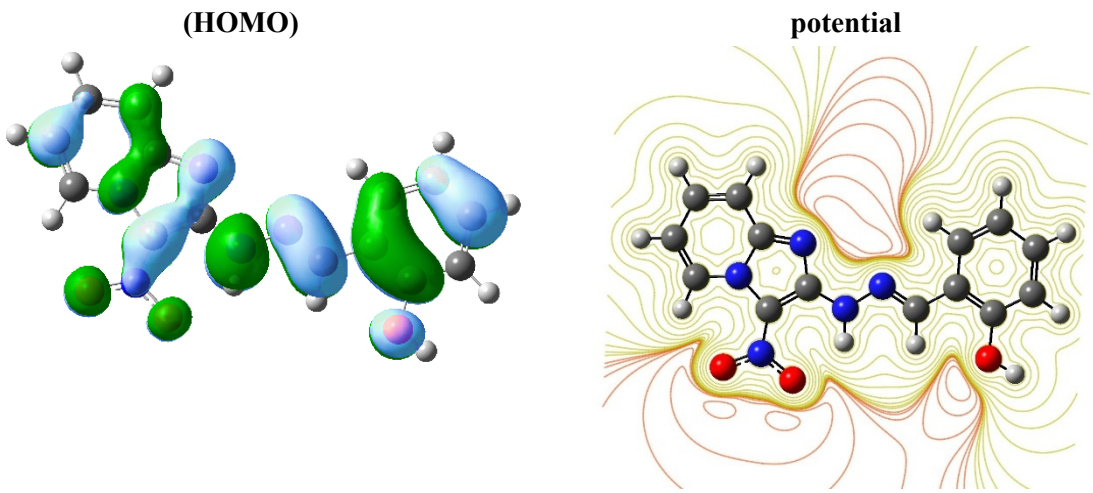


Figure 5. Frontier orbitals (HOMO and LUMO) and Electrostatic Potential (ESP) maps of 1-(3-nitroimidazo[1,2-a]pyridinyl)-3-(2-hydroxyphenyl)hydrazone, computed using DFT/B3LYP/6-311 G(d).

Quantum chemical calculations further provided the global and local reactivity descriptors compiled in Tables 4 and 5, respectively. The global descriptors for AKJ54 (Table 4) are in good agreement with reported literature values [37-40]. The high E_{HOMO} reflects the molecule's strong electron-donating ability, while the low E_{LUMO} indicates its capacity to accept electrons. Taken together, these frontier orbital energies point to a highly favorable reactivity for AKJ54, which is further corroborated by the narrow HOMO–LUMO energy gap (ΔE), indicative of efficient electron exchange with the environment. Additional parameters, namely electronegativity (χ), the global electrophilicity index (ω), and the fraction of electrons transferred (ΔN), offer complementary insights into the molecule's electron transfer capability. The elevated ω values confirm the electrophilic nature of this nitroimidazole–hydrazone derivative [41, 42]. The computed electron-withdrawing ability (4.324 eV) was used to derive ΔN; the resulting negative value suggests that electron transfer could proceed from the metal surface to the AKJ54 inhibitor in an adsorption process [39]. Collectively, these theoretical parameters provide a generally coherent rationale for the adsorption behavior observed in the thermodynamic analysis.

The identification of preferential reaction sites is consistent with previous reports [43, 44]. Based on the dual descriptor Δf_k, the most positive values denote regions susceptible to nucleophilic attack, whereas the most negative values indicate sites prone to electrophilic attack. As shown in Table 5, C7 and N29 atoms exhibit the highest Δf_k values, while C6 atom and the nitro group (N14, O15 and O16) show the lowest (most negative) values. Among all these atoms, nitrogen N29 (Δf_k = 0.069) and oxygen O16 (Δf_k = −0.102) are identified as the most likely sites for nucleophilic and electrophilic attack, respectively.

Table 4. Global reactivity descriptors of1-(3-nitroimidazo[1,2-a]pyridinyl)-3-(2-hydroxyphenyl)hydrazone

E_{HOMO} (eV)	E_{LUMO} (eV)	ΔE (eV)	E_T (ua)	χ (eV)	η (eV)	S (eV^{-1})	ω (eV)	ΔN
-5.907	-2.741	3.166	-1039.35	4.324	1.583	0.632	5.907	-0.014

Table 5. Fukui functions and dual descriptor of pertinent atoms of 1-(3-nitroimidazo[1,2-a]pyridinyl)-3-(2-hydroxyphenyl)hydrazone

Atom N°	q_k *(N+1)*	q_k *(N)*	q_k *(N-1)*	f_k^-	f_k^+	Δf_k
C1	0.459	0.454	0.420	0.005	0.034	-0.029
C2	0.202	0.188	0.161	0.014	0.027	-0.013
C3	-0.261	-0.282	-0.293	0.021	0.011	0.010
C4	-0.046	-0.057	-0.100	0.011	0.043	-0.032
C5	-0.111	-0.144	-0.160	0.033	0.016	0.017
C6	0.430	0.453	0.390	-0.023	0.063	**-0.086**
C7	0.625	0.583	0.602	0.042	-0.019	**0.061**
N12	-0.819	-0.819	-0.824	0	0.005	-0.005
N13	-0.317	-0.354	-0.371	0.037	0.017	0.020
N14	0.037	0.016	-0.064	0.021	0.080	**-0.059**
O15	-0.254	-0.328	-0.456	0.074	0.128	**-0.054**
O16	-0.320	-0.350	-0.482	0.030	0.132	**-0.102**
C17	0.101	0.043	-0.002	0.058	0.045	0.013
C19	-0.145	-0.112	-0.076	-0.033	-0.036	0.003
C20	0.273	0.218	0.186	0.055	0.032	0.023
C21	-0.028	-0.073	-0.11	0.045	0.037	0.008
C22	-0.127	-0.153	-0.168	0.026	0.015	0.011
C23	-0.144	-0.159	-0.160	0.015	0.001	0.014
C25	-0.089	-0.123	-0.147	0.034	0.024	0.010
N29	-0.559	-0.626	-0.624	0.067	-0.002	**0.069**
N31	-0.105	-0.125	-0.142	0.020	0.017	0.003
O32	-0.597	-0.632	-0.632	0.035	0	0.035

According to data from the literature [45–47], protonation, which is favored in acidic media, leads to the formation of cationic species. This process, resulting from the electrophilic attack of H^+ on the electron-rich heteroatoms of the molecule [48, 49], occurs preferentially on atoms with negative Δf_k values. Thus, an oxygen atom of the nitro group (N14, O15 and O16) is capable of protonation in the acidic medium considered, generating cations (Figure 6) that can be adsorbed onto the surface of the metal to be protected.

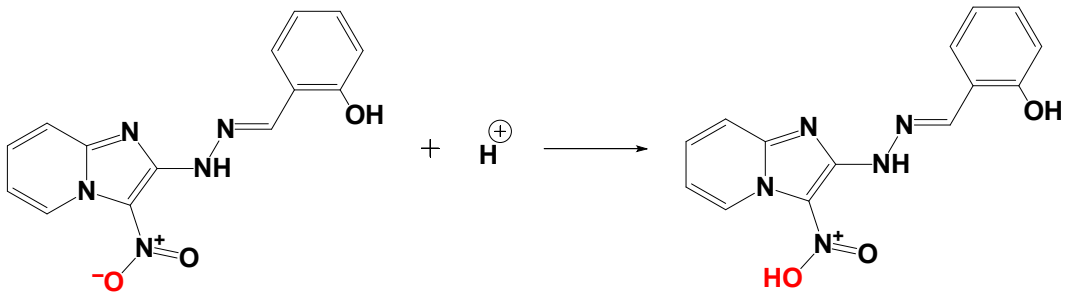


Figure 6. DFT-based preferential protonation of 1-(3-nitroimidazo[1,2-a]pyridinyl)-3-(2-hydroxyphenyl)hydrazone.

During the corrosion process, the Al^{3+} ions formed by metal oxidation promote the accumulation of Cl^- ions at the substrate surface [50]. The adsorbed Cl^- ions can then facilitate the adsorption of the protonated

imidazo[1,2-a]pyridine derivative, thereby slowing down the loss of the metal. This protonated inhibitorcould also compete with H^+ ions for adsorption sites or electrons at the metal surface, a behavior that has been proposed for organic inhibitors in HCl media [51, 52]. Protonated inhibitor species are known to adsorb electrostatically onto the negatively charged metal surface in HCl, which is consistent with a competitive interaction with H^+ at cathodic regions [53].

4. Conclusion

The present investigation revealed that the addition of 1-(3-nitroimidazo[1,2-a]pyridinyl)-3-(2-hydroxyphenyl)hydrazone at a concentration of 10^{-4} mol.L^{-1} to 1 M HCl effectively mitigated aluminum corrosion. The inhibitory action is governed by a mixed adsorption regime encompassing both physisorptive and chemisorptive interactions, leading to the formation of a surface barrier in which inhibitor species may adsorb at multiple sites and engage in lateral interactions. Elevated temperatures (303–323 K) induced partial desorption of the inhibitor, marginally compromising its otherwise outstanding inhibition efficiency of 91.91%. Complementary DFT calculations elucidated the adsorption mechanism, identifying the nitro group as the preferential site for protonation, thereby generating cationic species that contribute to the effective protection of the aluminum surface.

Funding

No funding was received during this research work.

Conflict of interest

The authors reported no potential conflict of interest.

Acknowledgment

The authors sincerely thank the reviewer for the valuable comments and constructive suggestions, which have significantly contributed to improving the quality and clarity of this manuscript.

References

[1] Arellanes-Lozada, P., Olivares-Xometl, O., Guzmán-Lucero, D., Likhanova, N. V., Domínguez-Aguilar, M. A., Lijanova, I. V., & Arce-Estrada, E. (2014). The inhibition of aluminum corrosion in sulfuric acid by poly(1-vinyl-3-alkyl-imidazolium hexafluorophosphate). *Materials, 7*(8), 5711–5734. https://doi.org/10.3390/ma7085711

[2] Dada, M., & Popoola, P. (2024). Recent advances in joining technologies of aluminum alloys: A review. *Discover Materials, 4*, Article 86. https://doi.org/10.1007/s43939-024-00155-w

[3] Singhal, V., Shelly, D., Babbar, A., Lee, S.-Y., & Park, S.-J. (2024). Review of wear and mechanical characteristics of Al-Si alloy matrix composites reinforced with natural minerals. *Lubricants, 12*(10), Article 350. https://doi.org/10.3390/lubricants12100350

[4] Kozina, F., Brodarac, Z. Z., Petrič, M., & Batič, B. Š. (2025). Degradation susceptibility of Al-2.18Mg-1.92Li alloy in severe environmental conditions. *Materials, 18*(9), Article 1938. https://doi.org/10.3390/ma18091938

[5] Abd El Aal, E. E., Abd El Wanees, S., Farouk, A., & Abd El Haleem, S. M. (2013). Factors affecting the

corrosion behaviour of aluminium in acid solutions. II. Inorganic additives as corrosion inhibitors for Al in HCl solutions. *Corrosion Science, 68*, 14–24. https://doi.org/10.1016/j.corsci.2012.09.038

[6] Davis, J. R. (1999). *Corrosion of aluminum and aluminum alloys*. ASM International.

[7] Dalbouha, A., & Rais, Z. (2022). Metal corrosion: In-depth analysis, economic impacts and inhibition strategies for enhanced infrastructure durability. *Journal of Applied Science and Environmental Studies, 5*(1), 13–21.

[8] Garhi, K., Chouicha, S., & Kelland, M. A. (2021). Field test investigation of the performance of corrosion inhibitors: A case study. *Journal of Petroleum Exploration and Production Technology, 11*(11), 3879–3888. https://doi.org/10.1007/s13202-021-01287-y

[9] Zakaria, H., Silai, Z., Hussain, G., Domblesky, J. P., Kong, J., Louhichi, B., & Wei, H. (2025). In-process and post-machining corrosion of aluminum alloys: Mechanisms, root causes, and inhibitive approaches. *Materials Today Chemistry, 48*, Article 102897. https://doi.org/10.1016/j.mtchem.2025.102897

[10] Verma, C., Ebenso, E. E., Quraishi, M. A., & Hussain, C. M. (2021). Recent developments in sustainable corrosion inhibitors: Design, performance and industrial scale applications. *Materials Advances, 2*(12), 3806–3850. https://doi.org/10.1039/D0MA00681E

[11] Zakeri, A., Bahmani, E., & Aghdam, A. S. R. (2022). Plant extracts as sustainable and green corrosion inhibitors for protection of ferrous metals in corrosive media: A mini review. *Corrosion Communications, 5*, 25–38. https://doi.org/10.1016/j.corcom.2022.03.002

[12] Salama, E. E., Alrashdi, S., Boraei, Ahmed T. A., Eid, S., Gomaa, I., Gad, E. S., Elhenawy, A. A., & Nady, H. (2025). Utilizing some indole derivatives to control mild steel corrosion in acidic environments: Electrochemical and theoretical methods. *Molecules, 30*(6), Article 1235. https://doi.org/10.3390/molecules30061235

[13] Assad, H., & Kumar, A. (2021). Understanding functional group effect on corrosion inhibition efficiency of selected organic compounds. *Journal of Molecular Liquids, 344*, Article 117755. https://doi.org/10.1016/j.molliq.2021.117755

[14] Al-Ahmed, Z. A. M., Kamel, M. M., Mahmoud, M. A. A., Ali, S. A. M., Ibrahim, A. Z., & Alshehri, B. M. (2025). 4-amino-5-(trifluoromethyl)-4H-1,2,4-triazole-3-thiol as an effective corrosion inhibitor for low carbon steel in HCl environment: Experimental and theoretical studies. *BMC Chemistry, 19*, Article 205. https://doi.org/10.1186/s13065-025-01553-8

[15] Quadri, T. W., Olasunkanmi, L. O., Akpan, E. D., Alfantazi, A., Obot, I. B., Verma, C., Al-Mohaimeed, A. M., Ebenso, E. E., & Quraishi, M. A. (2021). Chromeno-carbonitriles as corrosion inhibitors for mild steel in acidic solution: Electrochemical, surface and computational studies. *RSC Advances, 11*(5), 2462–2475. https://doi.org/10.1039/D0RA09590B

[16] Verma, C., Abdellattif, M. H., Alfantazi, A., & Quraishi, M. A. (2021). N-heterocycle compounds as aqueous phase corrosion inhibitors: A robust, effective and economic substitute. *Journal of Molecular Liquids, 340*, Article 117211. https://doi.org/10.1016/j.molliq.2021.117211

[17] Zaid, A. K., Merdas, S. M., & Hayal, M. Y. (2021). Heterocyclic compounds containing N atoms as corrosion inhibitors: A review. *Journal of Bioscience and Applied Research, 7*(2), 93–103. https://doi.org/10.21608/jbaar.2021.178505

[18] Baharin, N. A. N. K., Ghazali, S. A. I. S. M., Sirat, S. S., Tajuddin, A. M., Pungot, N. H., Normaya, E., Kamarudin, S. R. M., & Dzulkifli, N. N. (2024). In-depth investigation of corrosion inhibition mechanism: Computational, electrochemical, and theoretical studies of vanillin meldrum's acid on mild steel surface in 1 M HCl. *Journal of Molecular Liquids, 416*, Article 126390. https://doi.org/10.1016/j.molliq.2024.126390

[19] Kouamé, T. S., Ehouman, A. D., Akpataku, K. V., & Niamien, P. M. (2026). Inhibition of aluminum corrosion in hydrochloric acid medium by 2-(2-(4-chlorobenzylidene)hydrazinyl)-3-nitroimidazo[1,2-a]pyridine: Gravimetric

and adsorption studies. *Earthline Journal of Chemical Sciences, 13*(3), 231–244. https://doi.org/10.34198/ejcs.13326.18.231244

[20] Ahmed, S. K., Ali, W. B., & Khadom, A. A. (2019). Synthesis and investigations of heterocyclic compounds as corrosion inhibitors for mild steel in hydrochloric acid. *International Journal of Industrial Chemistry, 10*(2), 159–173. https://doi.org/10.1007/s40090-019-0181-8

[21] Ashmawy, A. M., Mostafa, M. A., Kamal, A. B., Ali, G. A. M., & El-Gaby, M. S. A. (2023). Corrosion inhibition of mild steel in 1 M HCl by pyrazolone-sulfonamide hybrids: Synthesis, characterization, and evaluation. *Scientific Reports, 13*, Article 18555. https://doi.org/10.1038/s41598-023-45659-2

[22] Xhanari, K., & Finšgar, M. (2016). Organic corrosion inhibitors for aluminium and its alloys in acid solutions: A review. *RSC Advances, 6*(67), 62833–62857. https://doi.org/10.1039/c6ra11818f

[23] Gummanar, N., Mokshanatha, P. B., Dyapur, P., & Yallappa, G. N. (2023). Organic corrosion inhibitors for aluminum-based alloys—A review. *Letters in Applied NanoBioScience, 12*(4), Article 170. https://doi.org/10.33263/LIANBS124.170

[24] Kouamé, T. S., Ehouman, A. D., Akpataku, K. V., & Niamien, P. M. (2026). Inhibition of aluminum corrosion in hydrochloric acid medium by 2-(2-(4-chlorobenzylidene)hydrazinyl)-3-nitroimidazo[1,2-a]pyridine: Gravimetric and adsorption studies. *Earthline Journal of Chemical Sciences, 13*(3), 231–244. https://doi.org/10.34198/ejcs.13326.18.231244

[25] Kouamé, T. S., Tigori, M. A., Allou, N. B., & Niamien, P. M. (2027). Study of 2-(2-benzylidenehydrazinyl)-3-nitroimidazo[1,2-a]pyridine for aluminum inhibition corrosion in 1 M hydrochloric acid. *International Journal of Chemistry, 19*(1), Article 15. https://doi.org/10.5539/ijc.v19n1p15

[26] Adingra, K. F., Alain, K., Coulibali, S., Etienne, C. T., Coulibaly, S., Ouattara, S., & Sissouma, D. (2022). Synthesis and anticandidosic activities of imidazo[1,2-a]pyridinehydrazone derivatives. *ChemXpress, 14*(1), Article 158. https://doi.org/10.37532/2320-1967.2022.14(1).169

[27] Koffi, A. A., Coulibaly, S., Yeo, M., Coulibaly, K. K., & Niamien, P. M. (2025). Delving ethyl 2-oxo-2H-chromene-3-carboxylate as a corrosion inhibitor for aluminum in acidic environments. *Oriental Journal of Chemistry, 41*(1), 57–65.

[28] Adingra, K. F., Alain, K., Coulibali, S., Etienne, C. T., Coulibaly, S., Ouattara, S., & Sissouma, D. (2022). Synthesis and anticandidosic activities of imidazo[1,2-a]pyridinehydrazone derivatives. *ChemXpress, 14*(1), Article 158. https://doi.org/10.37532/2320-1967.2022.14(1).169

[29] Ogunyemi, B. T., Latona, D. F., Ayinde, A. A., & Adejoro, I. A. (2020). Theoretical investigation to corrosion inhibition efficiency of some chloroquine derivatives using density functional theory. *Advanced Journal of Chemistry-Section A, 3*(4), 485–492. https://doi.org/10.33945/SAMI/AJCA.2020.4.10

[30] Husaini, M., Yunusa, U., Ibrahim, H. A., Usman, B., & Ibrahim, M. B. (2020). Corrosion inhibition of aluminium in phosphoric acid solution using glutaraldehyde as inhibitor. *Algerian Journal of Chemical Engineering, 1*, 12–21.

[31] Pan, J., Huang, X., Jiang, H., & Cao, K. (2026). 3-Hydroxy-2-naphthoylamide as corrosion inhibitor for carbon steel in 1 M HCl. *International Journal of Electrochemical Science, 21*(2), Article 101279. https://doi.org/10.20964/2026.02.101279

[32] Kokalj, A. (2023). On the use of the Langmuir and other adsorption isotherms in corrosion inhibition. *Corrosion Science, 217*, Article 111112. https://doi.org/10.1016/j.corsci.2023.111112

[33] He, J., Huang, H., & Zheng, X. (2026). Efficient and long-acting corrosion inhibition mechanisms and adsorption behavior of sodium laurate on AZ91D Mg alloy in oxalic acid solution. *Results in Surfaces and Interfaces, 24*, Article 100895. https://doi.org/10.1016/j.rsurfi.2026.100895

[34] Vaszilcsin, C. G., Putz, M. V., Kellenberger, A., & Dan, M. L. (2023). On the evaluation of metal–corrosion inhibitor interactions by adsorption isotherms. *Journal of Colloid and Interface Science, 639*, 274–292. https://doi.org/10.1016/j.jcis.2023.02.040

[35] Simonović, A. T., Žaklina, Z. T., Radovanović, M. B., Mihajlović, M. B. P., & Antonijević, M. M. (2020). Influence of 5-chlorobenzotriazole on inhibition of copper corrosion in acid rain solution. *ACS Omega, 5*(21), 12832–12841. https://doi.org/10.1021/acsomega.0c00553

[36] Yobo, G. J. M. V., Ehouman, A. D., Akpataku, K. V., & Niamien, P. M. (2026). Study of the protection of aluminum in hydrochloric acid (1 M) by 2-(1H-benzo[d]imidazol-2-yl)-3-phenylacrylonitrile: Gravimetric analysis and thermodynamic parameters. *Earthline Journal of Chemical Sciences, 13*(3), 245–257. https://doi.org/10.34198/ejcs.13326.19.245257

[37] Parlak, A. E., Omar, R. A., Koparir, P., & Salih, M. I. (2022). Experimental, DFT and theoretical corrosion study for 4-(((4-ethyl-5-(thiophen-2-yl)-4H-1,2,4-triazole-3-yl)thio)methyl)-7,8-dimethyl-2H-chromen-2-one. *Arabian Journal of Chemistry, 15*(5), Article 104088. https://doi.org/10.1016/j.arabjc.2022.104088

[38] Abdelsalam, M. M., Bedair, M. A., Hassan, A. M., Heakal, B. H., Younis, A., Elbialy, Z. I., Badawy, M. A., Fawzy, H. El-D., & Fareed, S. A. (2022). Green synthesis, electrochemical, and DFT studies on the corrosion inhibition of steel by some novel triazole Schiff base derivatives in hydrochloric acid solution. *Arabian Journal of Chemistry, 15*(1), Article 103491. https://doi.org/10.1016/j.arabjc.2021.103491

[39] Esan, T. O., Oyeneyin, O. E., Olanipekun, A. D., & Ipinloju, N. (2022). Corrosion inhibitive potentials of some amino acid derivatives of 1,4-naphthoquinone—DFT calculations. *Advanced Journal of Chemistry-Section A, 5*(4), 263–270.

[40] Lin, B.-l., Zhou, X.-x., Duan, T.-h., Zhao, C., Zhu, J.-h., & Xu, Y.-y. (2024). Experimental and theoretical study on corrosion inhibition and adsorption performance of Ipomoea batatas L. leaf extract for mild steel. *Arabian Journal of Chemistry, 17*(2), Article 105410. https://doi.org/10.1016/j.arabjc.2023.105410

[41] Alaoui, A. O., Elfalleh, W., Hammouti, B., Titi, A., Messali, M., Kaya, S., Ibrahimi, B. EL., & El-Hajjaji, F. (2025). Theoretical prediction of corrosion inhibition by ionic liquid derivatives: A DFT and molecular dynamics approach. *RSC Advances, 15*(16), 12645–12652. https://doi.org/10.1039/d5ra01097g

[42] Azeez, Y. H., Mamand, D. M., Omer, R. A., Awla, A. H., & Omar, K. A. (2024). Investigation of corrosion inhibition and adsorption properties of quinoxaline derivatives on metal surfaces through DFT and Monte Carlo simulations. *Corrosion Reviews, 42*(6), 775–793. https://doi.org/10.1515/corrrev-2024-0007

[43] Oyeneyin, O. E., Ojo, N. D., Ipinloju, N., Agbafa, E. B., & Emmanuel, A. V. (2022). Investigation of the corrosion inhibition potentials of some 2-(4-(substituted) arylidene)-1H-indene-1,3-dione derivatives: Density functional theory and molecular dynamics simulation. *Beni-Suef University Journal of Basic and Applied Sciences, 11*, Article 132. https://doi.org/10.1186/s43088-022-00312-3

[44] Oyeneyin, O. E. (2023). DFT and Monte Carlo simulations on the corrosion inhibitive potentials of some furan-based carbohydrazide derivatives. *Letters in Applied NanoBioScience, 12*(4), Article 113. https://doi.org/10.33263/LIANBS124.113

[45] Abeng, F. E., Evo, S. E., Mathias, G. E., Ikenyirimba, O. J., Thakur, A., Anadebe, V. C., Mothudi, B. M., & Ebenso, E. E. (2026). Corrosion inhibition mechanism of Eupatorium capillifolium extract on mild steel: Insight from experimental and molecular dynamics simulations. *Results in Surfaces and Interfaces, 23*, Article 100811. https://doi.org/10.1016/j.rsurfi.2026.100811

[46] Sedik, A., Athmani, S., Saoudi, A., Ferkous, H., Ribouh, N., Lerari, D., Bachari, K., Djellali, S., Berredjem, M., Solmaz, R., Alam, M., Jeon, B.-H., & Benguerba, Y. (2022). Experimental and theoretical insights into copper corrosion inhibition by protonated amino-acids. *RSC Advances, 12*(36), 23718–23735. https://doi.org/10.1039/d2ra03535a

[47] Mouats, N., Djellali, S., Ferkous, H., Sedik, A., Delimi, A., Boublia, A., Rachedi, K. O., Berredjem, M., Çukurovali, A., Alam, M., Ernsti, B., & Benguerba, Y. (2024). Comprehensive investigation of the adsorption, corrosion inhibitory properties, and quantum calculations for 2-(2,4,5-trimethoxybenzylidene) hydrazine carbothioamide in mitigating corrosion of XC38 carbon steel under HCl environment. *ACS Omega, 9*(26), 27945–27962. https://doi.org/10.1021/acsomega.3c10240

[48] Abdel-karim, A. M., Azzam, R. A., Shehata, O. E. S., Adly, M. A., El-Shamy, O. A. A., & El Mahdy, G. A. (2025). Electrochemical performance of a novel 1-(benzo[d]thiazol-2-yl)-3-methylguanidine as effective corrosion inhibitor for carbon steel in 1 M hydrochloric acid. *Scientific Reports, 15*, Article 28196. https://doi.org/10.1038/s41598-025-12838-2

[49] Matine, A., Es-Sounni, B., Bakhouch, M., Bahkali, A. H., Abdallaoui, H. E. A. E., Wang, S., Syed, A., Wong, L. S., Saleh, N., & Zeroual, A. (2024). Design, synthesis, and evaluation of a pyrazole-based corrosion inhibitor: A computational and experimental study. *Scientific Reports, 14*, Article 25238. https://doi.org/10.1038/s41598-024-76300-5

[50] Gadow, H. S., Abd El-Monem, N. M., & El-Settawy, R. M. (2026). Use of Swiss chard stems and green pea peel extracts as anticorrosive agents for aluminum in 1 M HCl. *RSC Advances, 16*(6), 4959–4992. https://doi.org/10.1039/d5ra09501h

[51] Ansari, K. R., & Quraishi, M. A. (2015). Effect of three component (aniline–formaldehyde and piperazine) polymer on mild steel corrosion in hydrochloric acid medium. *Journal of the Association of Arab Universities for Basic and Applied Sciences, 18*(1), 12–18. https://doi.org/10.1016/j.jaubas.2014.04.001

[52] Prajapati, K. G., & Desai, P. S. (2026). Corrosion inhibition of aluminum in HCl by amine derivatives: Experimental and computational evaluation. *Next Materials, 13*, Article 102748. https://doi.org/10.1016/j.nxmate.2026.102748

[53] Kamboj, V., Bhushan, B., Kumar Singh, M. K., Nayak, A., Rastogi, C., Mangla, B., & Ji, G. (2026). Investigation on the working mechanisms of sustainable corrosion inhibitors for mild steel in acid solutions: A review based on experimental and computational analysis. *Surface Science and Technology, 4*, Article 13. https://doi.org/10.1007/s44251-025-00119-z

This is an open access article distributed under the terms of the Creative Commons Attribution License (http://creativecommons.org/licenses/by/4.0/), which permits unrestricted, use, distribution and reproduction in any medium, or format for any purpose, even commercially provided the work is properly cited.